Optics Communications 418 (2018) 93–97

Contents lists available at ScienceDirect

Optics Communications

journal homepage: www.elsevier.com/locate/optcom

Experimental demonstration of PAM-DWMT for passive optical network

Bangjiang Lin [a,*], Kaiwei Zhang [b], Xuan Tang [a,*], Zabih Ghassemlooy [c], Chun Lin [b], Zhenlei Zhou [b]

[a] Quanzhou Institute of Equipment Manufacturing, Haixi Institutes, Chinese Academy of Sciences, Quanzhou, 362200, China
[b] State Key Laboratory of Advanced Optical Communication Systems and Networks, Peking University, 100871, China
[c] Optical Communications Research Group, NCRLab, Faculty of Engineering and Environment, Northumbria University, NE1 8ST, Newcastle, UK

ARTICLE INFO

Keywords:
Passive optical network (PON)
Discrete wavelet multitone (DWMT)
Pulse amplitude modulation (PAM)

ABSTRACT

We experimentally demonstrate a discrete wavelet multitone (DWMT) modulation scheme based on pulse amplitude modulation (PAM) for next generation passive optical network (PON), which offers high tolerance against chromatic dispersion, high spectral efficiency, low peak to average power ratio (PAPR) and low side lobes. The experimental results show the chromatic dispersion induced power penalties are negligible after 20km fiber transmission. Compared with orthogonal frequency division multiplexing (OFDM), DWMT offers a better receiver sensitivity.

1. Introduction

Passive optical network (PON) regarded as the best solution for access network has been widely deployed in the worldwide, due to its high speed and low cost [1,2]. As the demand for broadband services increases rapidly, orthogonal frequency division multiplexing (OFDM)-based PON has been considered as a promising candidate for next generation PON, because of its flexible resource allocation both in time and frequency domains, high spectral efficiency, and strong tolerance to fiber dispersion [3–5]. However, OFDM-PON has some drawbacks. OFDM is a discrete Fourier transform (DFT) based multicarrier modulation scheme which convert a high speed data stream into a number of sub-streams with lower data rate. Due to the rectangular shaped DFT window, the OFDM signal has high side lobes, which induces out of band radiation. In addition, a cyclic prefix is required to avoid the inter symbol interference (ISI) caused by fiber dispersion, which reduces its spectrum efficiency. Finally, the OFDM signal is characterized by high peak to average power ratio (PAPR) which requires much stringent linearity for any post- and pre-amplifiers to avoid excessive inter-modulation distortion [6]. This would increase the cost of deployed PON architecture, especially for cost-sensitive optical network units (ONUs).

In this paper, we propose a discrete wavelet multitone (DWMT) modulation scheme for PON, which provides all the advantages known in OFDM-PON and also provides some excellent features such as low side lobes, low PAPR, and improved spectrum efficiency due to the removal of cyclic prefix (CP). The DWMT modulation has been standardized in IEEE 1901 for power line communication [7], and also been widely investigated as a good candidate for digital subscriber loop (DSL) [8], wireless communications [9–11], optical communications [12]. To the best of our knowledge, this is the first work investigate the DMWT modulation as a promising solution for next generation PON. The feasibility of DWMT-PON is verified with experiment demonstration. As shown in our experiment, the DWMT offers strong tolerance against the chromatic dispersion and better receiver sensitivity compared with the OFDM. In [13], filter bank multicarrier (FBMC) based modulation scheme has been proposed for PON, which can also operate without a CP and has low side lobes. Compared with the FBMC based PON system, our propose scheme offers comparative tolerance against the chromatic dispersion, lower PAPR and lower complexity.

The rest of the paper is organized as follows. Section 2 describes the proposed DWMT scheme for PON in detail. The experiment setup and results for the DWMT-PON are given in Section 3. Section 4 presents the concluding remarks.

2. DWMT

Wavelets are waveforms with limited duration and an average value of zero. There are numerous pre-defined wavelets that can be used in signal analysis, which divides a signal into its frequency components with a resolution based on the scale of the wavelet, and produce coefficients that are an indication of correlation between the wavelet and the signal under investigation at a particular time and scale. One of the key features of wavelet transform is that it produces results

* Corresponding authors.
E-mail addresses: linbangjiang@163.com (B. Lin), xtang@fjirsm.ac.cn (X. Tang).

https://doi.org/10.1016/j.optcom.2018.02.070
Received 8 November 2017; Received in revised form 16 January 2018; Accepted 28 February 2018
0030-4018/© 2018 Elsevier B.V. All rights reserved.

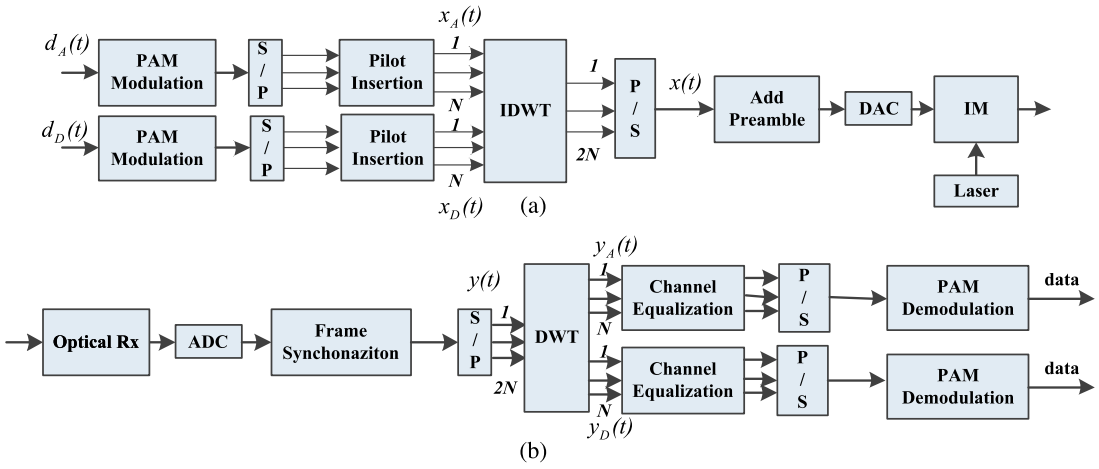

Fig. 1. Block diagram of (a) transmitter and (b) receiver for PAM-DWMT-PON.

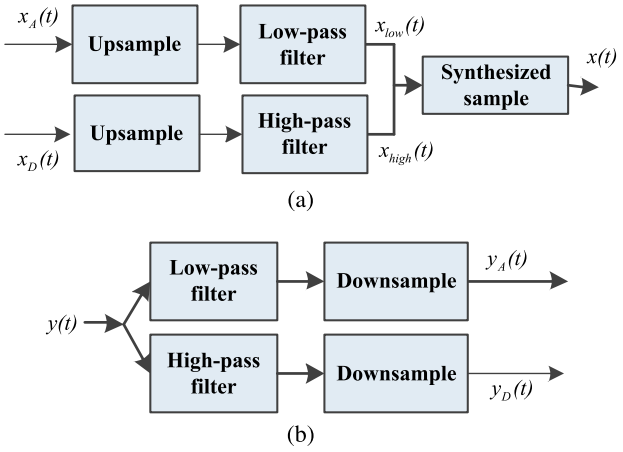

Fig. 2. Block diagram of (a) IDWT and (b) DWT.

that are related to time, which give an indication of not only what frequencies (scales) a signal contains but also when it appear. This should be contrasted against basic Fourier analysis that produces values relating purely to the frequency. Discrete wavelet transform (DWT) are computationally efficient with reduced simulation time compared to continuous wavelet. It involves using successive, complementary low-pass filter (LPF) and high-pass filter (HPF) to form the filters bank, which split the signal into its approximation and detail coefficients. The filter bank level depends on the bandwidth availability. With traditional digital filtering this would leave us with two signals both with the same number of sample points as the original. The signal resolution, which is a measure of detailed information of the signal, is converted by the filtering and scale process. Down sampling of signals by a factor of 2 is used to remove multiple signal samples. Up sampling signal is used to increase rate by adding new samples to the signal. Both DWT and inverse discrete wavelet transform (IDWT) are given by:

$$s_n^m = \int s(t)\, 2^{\frac{m}{2}} \psi\left(2^m t - n\right) dt, \tag{1}$$

$$s(t) = \sum_{m=-\infty}^{\infty} \sum_{n=-\infty}^{\infty} s_n^m 2^{\frac{m}{2}} \psi\left(2^{\frac{m}{2}} t - n\right), \tag{2}$$

where ψ is the wavelet kernel and is selected based on the mother wavelet chosen. Note that, IDWT is used to reconstruct signal process.

3. Proposed PAM-DWMT scheme for PON

Fig. 1 shows the block diagrams for the transmitter (Tx) and receiver (Rx) for PAM-DWT-PON. At the Tx, the binary data stream $d_A(t)$ and $d_D(t)$ are mapped to pulse amplitude modulation (PAM) symbols respectively prior to serial to parallel conversion. Then pilots are inserted for the purpose of channel estimation. The inverse discrete wavelet transform (IDWT) requires two parts of input data. $x_A(t)$ is regarded as the approximation part, while $x_D(t)$ are inserted as the detail part. The lengths of the approximation and detail part are both N, which is an integer power of 2. The IDWT consist of quadrature mirror filter (QMF) bank that consists of half-band LPF with an impulse response $h(t)$ and half-band HPF with an impulse response of $g(t)$, which is shown in Fig. 2(a). The approximation part $x_A(t)$ and the detail part $x_D(t)$ are up sampled by a factor of 2 and passed through the LPF and HPF, respectively. The output of which can be written as:

$$\begin{aligned} x_{low}(t) &= x_A(t) \otimes h(t) \\ x_{high}(t) &= x_D(t) \otimes g(t), \end{aligned} \tag{3}$$

where $\otimes$ demotes convolution operation. These filtered streams are then summed and constitute a wavelet symbol $x(t)$. To reassemble the reconstructed signal perfectly at the Rx in the absence of encoding, quantization and transmission errors, an orthonormal perfect reconstruction (OPR) requirement usually applies for the two filters. The OPR condition is given as:

$$g(n) = (-1)^n h(L-1-n), \tag{4}$$

$$g^T g = 1, \tag{5}$$

$$\sum_{n=-\infty}^{\infty} g(n)g(n+2k) = \delta(k), \tag{6}$$

where g is the vector from of $g(n)$, L is the length of $h(n)$. The preamble is added in the front of each frame for the purpose of synchronization, which includes a real-value Chu sequence. A digital-to-analog converter (DAC) is used to convert the digital signal into analog signal. The generated PAM-DWMT signal is real-valued, which can be used for intensity modulation (IM) of the laser. After IM, the optical PAM-DWMT signal is fed into the distribution network. At the Rx, the optical signal is firstly detected by a photo detector, and the output of which is converted into a digital format using an analog-to-digital converter (ADC). After frame synchronization, the received signal is passed through serial-to-parallel conversion. Then the received signal $y(t)$ is passed through an DWT with a LPF and a HPF, which have an impulse response of $h^*(t)$ and $g^*(t)$, respectively. Note that $h^*(t)$ and $g^*(t)$ are the conjugates of $h(t)$ and $g(t)$, respectively. The outputs of the LPF and HPF are then down sampled with a factor of 2, respectively, as shown in Fig. 2(b). The pilots

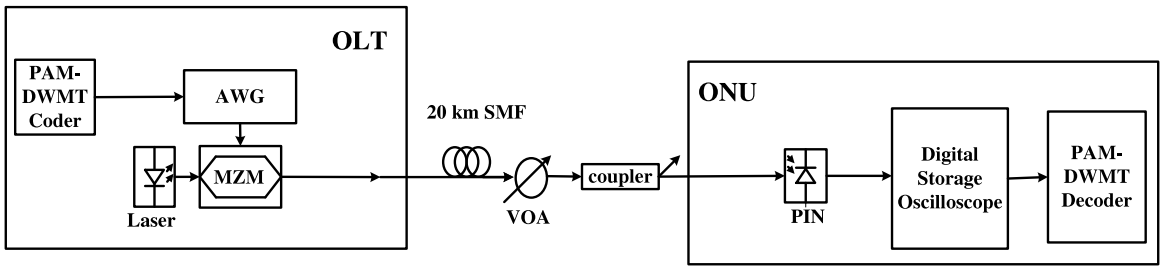

Fig. 3. Experiment setup of PAM-DWMT-PON (MZM: Mach–Zehnder modulator, SMF: single mode fiber, AWG: arbitrary waveform generator, VOA: variable optical attenuator).

are separated from the received approximation part $y_A(t)$ and detail part $y_d(t)$, which are used to calculate the channel coefficient. After channel equalization, the received signals are fed into the PAM demodulation module to recover the transmitted binary data, respectively.

4. Experiment setup and results

The experimental setup for the PAM-DWMT based PON is shown in Fig. 3. The PAM-DWMT signal is firstly generated in the Matlab domain, the detail modulation process of which can be found in Fig. 1(a). The generated signal is uploaded into an arbitrary waveform generator (AWG) with a sampling rate of 10 GS/s, the output of which is used for intensity modulation of a laser using a Mach–Zehnder modulator (MZM). Note that digital to analog conversion is included in AWG. PAM with four levels is applied and the size of N is set to 256. Harr wavelet is used to decompose and reconstruct the signal. Haar functions have been used from 1910 when they were introduced by the Hungarian mathematician Alfred Haar. The Haar function, being an odd rectangular pulse pair, is the simplest and oldest orthonormal wavelet with compact support [14]. The Harr wavelet function can be described as follows:

$$\psi(t) = \begin{cases} 1 & 0 \le t \le 0.5 \\ -1 & 0.5 \le t \le 1 \\ 0 & \text{otherwise.} \end{cases} \tag{7}$$

The filter coefficients while using Harr wavelet are given by:

$$h(n) = \frac{1}{\sqrt{2}}(-1, 1), g(n) = \frac{1}{\sqrt{2}}(1, 1). \tag{8}$$

The wavelength and the transmitted power are 1550 nm and 10 dBm, respectively. The optical PAM-DWMT signal is fed into the distribution network, which is emulated with a single mode fiber, a variable optical attenuator (VOA) and a 50/50 coupler. At the ONU side, the optical signal is firstly detected by a photo-detector and then passed through an ADC (this is included in the digital scope). The captured digital signal is recorded on a real-time digital oscilloscope. Then the received signal is offline processed in order to recover the transmitted data as shown in Fig. 1(b). All the key system parameters adopted in this work are depicted in Table 1.

Figs. 4 and 5 show the BER performance under back to back, 20 km and 80 km fiber for the approximation and detail parts of PAM-DWMT respectively. As shown in Fig. 4, the chromatic dispersion induced power penalties after 20 km and 80 km fiber are negligible for the approximation part. Whereas at the BER of 1e−3, the power penalties after 20 km and 80 km fiber are negligible and about 2.5 dB for the detail part. This is because the high frequency band suffers from more double sideband (DSB) power fading induced by chromatic dispersion [15,16]. Wavelet transform belongs to the family of overlapped transforms, i.e. the beginning of a symbol is transmitted before the previous one ends. The inter-symbol orthogonality is maintained due to the shift orthogonal property of the waveforms [17]. This overlapping feature increases the symbol duration and hence yields a better spectral

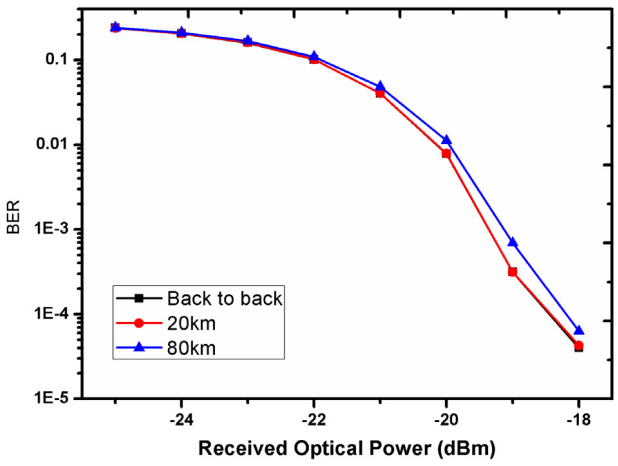

Fig. 4. BER performance for the approximation part of PAM-DWMT.

containment along with higher dispersion tolerance. On the other hand, because of the overlapping of the symbols in time domain, CP is not available for wavelets.

For comparison, an OFDM-based PON is also considered here, the experimental setup of which is similar with that of PAM-DWMT. The differences between them are the coder and decoder in the Matlab domain. In OFDM-PON, the DFT and CP sizes are 256 and 8, respectively. In order to generate a real-valued OFDM signal, Hermitian symmetry is applied to the signal prior to IDFT. Both the 0th and 128th subcarriers carry no data, whereas 1–127th subcarriers are used for data transmission, and 129–255th subcarriers carry the complex conjugate of data on the 1–127th subcarriers. Quadrature phase shift keying is used and the sampling rate of AWG is set to 10 GS/s. The bit rates of PAM-DWMT and QPSK-OFDM are 10 Gb/s and 9.62 Gb/s, respectively. Due to the insertion of CP, QPSK-OFDM has lower bit rate compared with PAM-DWMT using the same bandwidth.

Fig. 6 shows the PAPR comparison of QPSK-OFDM and PAM-DWMT. The detail parameters for QPSK-OFDM and PAM-DWMT modulation can be found in Table 1. As illustrated in Fig. 6, the PAM-DWMT has much lower PAPR than QPSK-OFDM. Fig. 7 shows the BER performances of QPSK-OFDM and PAM-DWMT after 20 km fiber transmissions. Figs. 8 and 9 show the received electrical power spectrum for DWMT and OFDM after 20 km fiber transmission with a received optical power of 0 dBm, respectively. The BER for the PAM-DMT is calculated from the average of the approximation and detail parts. The chromatic dispersion induced power penalties are negligible after 20 km fiber transmission for both QPSK-OFDM and PAM-DWMT, as shown in Figs. 8 and 9. Compared with QPSK-OFDM, PAM-DWMT offers better receiver

Table 1
System parameters.

Parameter	Value
• AWG sampling rate	10 GS/s
• Scope sampling rate	10 GS/s
• Transmit optical power	10 dBm
• Propagation distance	20, 80 km
OFDM	
• DFT size	256
• CP size	8
• Modulation format	QPSK
• Bit rate	9.62 Gb/s
PAM-DWMT	
• Wavelet	Haar
• Modulation format	4-PAM
• Bit rate	10 Gb/s

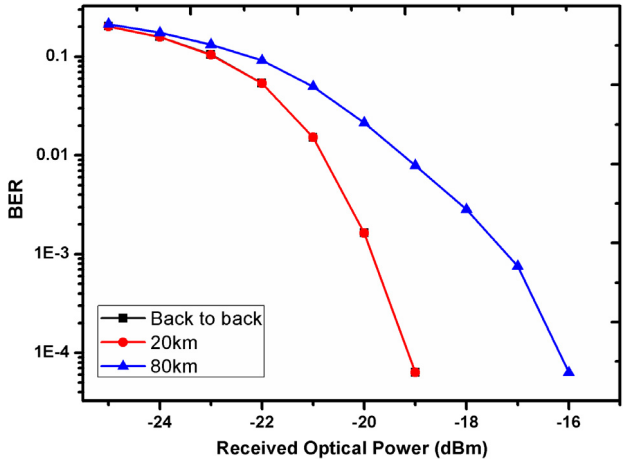

Fig. 5. BER performance for the detail part of PAM-DWMT.

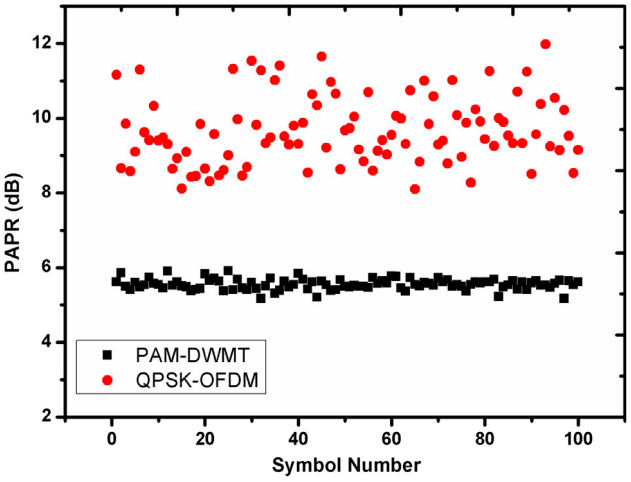

Fig. 6. PAPR comparison between QPSK-OFDM and PAM-DWMT.

sensitivity owing to its low PAPR and low side lobes. The receiver sensitivity is defined as the required received power to achieve a BER of 1e−3.

5. Conclusion

In this paper, we proposed an experimental demonstration of PAM-DWMT for next generation PON, which offered high tolerance against chromatic dispersion, high spectral efficiency, low PAPR and low side lobes. We showed that the chromatic dispersion induced power penalties after 20 km and 80 km fiber were negligible for the approximation part. Whereas at the BER of 1e−3, the power penalties after 20 km and 80 km

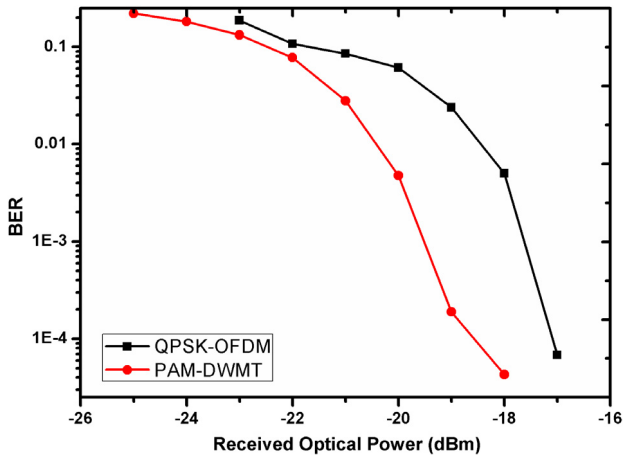

Fig. 7. BER performances of QPSK-OFDM and PAM-DWMT after 20 km fiber transmission.

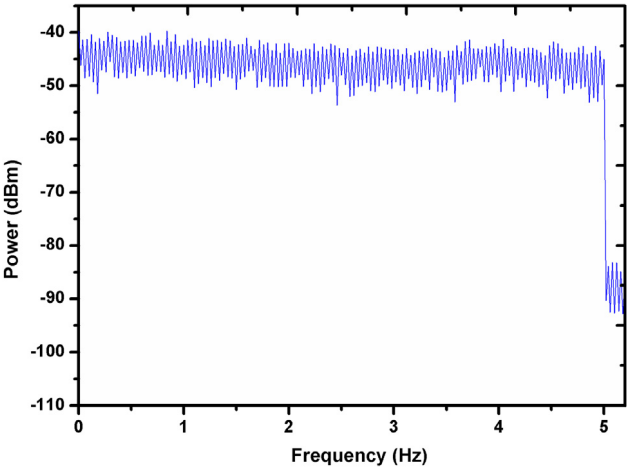

Fig. 8. Received electrical power spectrum for DWMT after 20 km fiber transmission with a received optical power of 0-dBm.

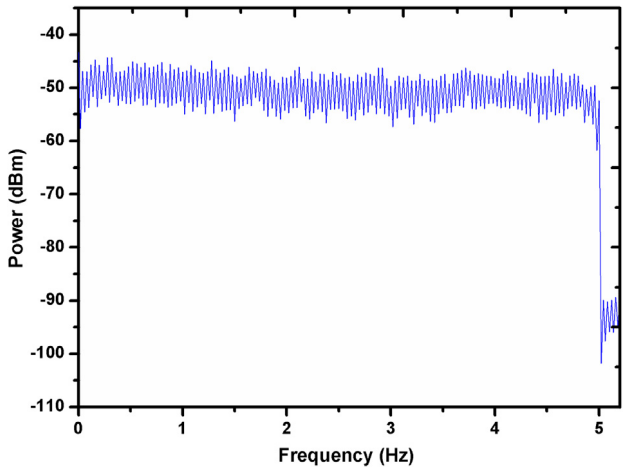

Fig. 9. Received electrical power spectrum for OFDM after 20 km fiber transmission with a received optical power of 0-dBm.

fiber were negligible and about 2.5 dB for the detail part. Compared with the OFDM scheme, the PAM-DWMT offered a lower PAPR and better receiver sensitivity after 20 km fiber transmission.

Acknowledgments

This work was supported in part by the National Science Foundation of China under Grant 61601439 and 61501427, in part by the Chunmiao Project of Haixi Institutes, Chinese Academy of Sciences, in part by Fujian Science Foundation under Grant 2017J05111, in part by External Cooperation Program of Chinese Academy of Sciences under Grant 121835KYSB20160006, in part by Program of Quanzhou Science and Technology under Grant 2016G007 and 2016T010.

References

[1] Chang-Hee Lee, W.V. Sorin, B.Y. Kim, Fiber to the home using a PON infrastructure, J. Lightwave Technol. 24 (12) (2006) 4568–4583.
[2] Bangjiang Lin, Juhao Li, Yuanbao Luo, Yangsha Wan, Yongqi He, Zhangyuan Chen, Symmetric 4 × 25-Gb/s DSP-enhanced TWDM-PON with DSB modulation and RSOA, IEEE Photon. Technol. Lett. 26 (21) (2014) 2103–2106.
[3] Bangjiang Lin, Xuan Tang, Yiwei Li, Shihao Zhang, Time-domain channel estimator for polarization interleaving direct-detection orthogonal frequency-division multiplexing passive optical network, Opt. Eng. 55 (6) (2016) 066107.
[4] D. Qian, N. Cvijetic, J. Hu, T. Wang, 108 Gb/s OFDMA-PON with polarization multiplexing and direct-detection, in: Proceedings of Optical Fiber Communication Conference, OFC, 2009, paper PDPD5.
[5] Cvijetic Neda, Dayou Qian, Junqiang Hu, Ting Wang, Orthogonal frequency division multiple access PON (OFDMA-PON) for colorless upstream transmission beyond 10 Gb/s, IEEE J. Sel. Areas Commun. 28 (6) (2010) 781–790.
[6] Hui Yang, Juhao Li, Bangjiang Lin, Song Jiang, Yongqi He, Zhangyuan Chen, Cost-effective upstream scheme for the next-generation PON based on interleaved frequency-division multiple access, IEEE Photon. Technol. Lett. 24 (9) (2012) 784–786.
[7] H.C. Ferreira, L. Lampe, J. Newbury, T.G. Swart, Power Line Communications: Theory and Applications for Narrowband and Broadband Communications over Power Line, John Wiley & Sons, 2010.
[8] A. Khan, C.H. Seong, D.R. Jeong, S.Y. Shin, Impact of impulse noise on DWMT transceiver with overlap FD, in: Proceedings of International Symposium on Intelligent Signal Processing and Communication Systems, IEEE, 2016, pp. 574–579.
[9] A. Mannan, A. Habib, Adaptive processing of image using DWT and FFT OFDM in AWGN and Rayleigh channel, in: Proceedings of International Conference on Communication, Computing and Digital Systems, IEEE, 2017, pp. 346–350.
[10] K. Chen, T. Chiueh, A cognitive radio system using discrete wavelet multitone modulation, IEEE Trans. Circuits Syst. I. Regul. Pap. 55 (10) (2008) 3246–3258.
[11] N. Hariprasad, G. Sundari, Performance comparison of DWT OFDM and FFT OFDM in presence of CFO and doppler effect, in: Proceedings of International Conference on Control, Instrumentation, Communication and Computational Technologies, IEEE, 2014, pp. 567–570.
[12] Li An, W. Shieh, R.S. Tucker, Wavelet packet transform-based OFDM for optical communications, J. Lightwave Technol. 28 (24) (2010) 3519–3528.
[13] Saljoghei Arsalan, et al., Filter Bank Multicarrier (FBMC) for long-reach intensity modulated optical access networks, Opt. Commun. 389 (2017) 110–117.
[14] Radomir S. Stanković, Bogdan J. Falkowski, The Haar wavelet transform: its status and achievements, Comput. Electr. Eng. 29 (1) (2003) 25–44.
[15] Bangjiang Lin, Juhao Li, Hui Yang, Yangsha Wan, Yongqi He, Zhangyuan Chen, Comparison of DSB and SSB transmission for OFDM-PON, IEEE J. Opt. Commun. Netw. 4 (11) (2012) B94–B100 (invited).
[16] L. Zhang, Q. Zhang, T. Zuo, Z. Zhou, G.N. Liu, X. Xu, C-band single wavelength 100-Gb/s IM-DD transmission over 80-km SMF without CD compensation using SSB-DMT, in: Proceedings of Optical Fiber Communication Conference, OFC, 2015, pp. 1–3.
[17] Omer Bulakci, et al., Wavelet transform based optical OFDM, in: Conference on IEEE Optical Fiber Communication — Incudes Post Deadline Papers, 2009, OFC 2009, 2009, pp. 1–3.